The evolution of red blood cell shape in a continental radiation of fishes

Brenda Oliveira Martins[1*], Lilian Franco-Belussi[2*], Mayara Schueroff Siqueira[2], Carlos E. Fernandes[2], Diogo B. Provete[2,3]

[1] *Graduate Program in Animal Biology. Instituto de Biociências, Universidade Federal de Mato Grosso do Sul, Campo Grande, Mato Grosso do Sul, 79002970, Brasil.* brendabernini@gmail.com

[2] *Instituto de Biociências, Universidade Federal de Mato Grosso do Sul, Campo Grande, Mato Grosso do Sul, 79002970, Brasil.* lilian.belussi@gmail.com; carlos.fernandes@ufms.br; mayara_schueroff@hotmail.com

[3] *Gothenburg Global Biodiversity Centre, Göteborg, Box 100, S 405 30, Sweden.*

[*]These authors contributed equally to this work

Short running title: RBC shape in fishes

Author contributions: BOM collected cell morphometric data assisted by MSS, LFB. CEF and DBP conceived the study. DBP analysed and curated the data. DBP, LFB, and BOM prepared the first draft of the manuscript to which all authors contributed afterwards.

Corresponding author:

Diogo B. Provete
e-mail: diogo.provete@ufms.br
Instituto de Biociências - INBIO
Universidade Federal de Mato Grosso do Sul – UFMS, Av. Costa e Silva, s/n, Bairro Universitário, Campo Grande, 79002-970, Mato Grosso do Sul, Brasil

Abstract

The size and shape of Red Blood Cells (RBC) can provide key information on life history strategies in vertebrates. However, little is known about how RBC shape evolved in response to environmental factors and the role of phylogenetic relationship. Here, we analyzed RBC morphometrics in a continental radiation of fishes testing the hypothesis that phylogenetic relationship determines species occupation of morphospace. We collected blood samples of five specimens of 15 freshwater fish species from six orders and used basic stereological methods to measure cell and nucleus area, perimeter, and diameter, cell and nucleus volume, nucleus:cytoplasm ratio, and shape factor of 50 cells per specimen. Then, we conducted a phylogenetic Principal Components Analysis using a dated phylogeny and built a phylomorphospace. To test if the phylogenetic relationship predicted the phenotypic similarity of species, we calculated multivariate phylogenetic signal. We also estimated the evolution rate of RBC shape for each node and tip using ridge regression. Finally, we tested if the position in the water column influenced RBC shape using a phylogenetic GLS. RBC shape seems to have evolved in a non-stationary way because the distribution pattern of species in the phylomorphospace is independent of the phylogeny. Accordingly, the rate of evolution for shape was highly heterogeneous, with an increase in the genus *Pygocentrus*. Water column position does not influence RBC shape. In conclusion, RBC shape seem to have evolved in response to multiple selective pressures independent of life history characters.

Key-words: phylomorphospace, erythrocytes, stereology, phylogenetic signal, rate of evolution.

Introduction

The shape, size, and number of Red Blood Cells (RBC) vary greatly in vertebrates (Wintrobe 1934). Although the reasons for this variation are not well understood, phylogenetic relationships can at least partially explain it, because early diverging vertebrate lineages have larger but fewer RBC (Anderson et al., 2018). Early diverging vertebrates also have round and flattened RBCs with a central nucleus, while derived lineages have ellipsoid cells (Nikinmaa 1990; Glomski et al. 1992).

Both abiotic factors and life history traits can also affect the composition and morphology of fish RBC (Dal'Bó et al., 2015; Kumar, 2016; Yakhnenko et al., 2016). For example, RBC size is inversely related to swimming ability in teleosts (Lay and Baldwin 1999; Witeska 2013), while size of RBCs is highest at intermediate altitude in one lizard species (González-Morales et al. 2017). In addition, cell size has an inverse relation with metabolic rate, suggesting lowest metabolic cost to maintain active membrane transport in large cells (Szarki, 1970; Graham et al. 1985, Maciak et al, 2011). Deep-sea fish species have large RBC, compatible with their low metabolism (Graham et al. 1985). Then, RBC size in teleost has an adaptative value and changes in response to external factors (Lay and Baldwin 1999). RBC volume is another morphological variable correlated with physiological state in fish. For example, cell volume is negative correlated with hemoglobin concentration, while nuclear volume explains only 17% of cell volume (Lay and Baldwin 1999).

The nucleus of RBC is strongly related to species adaptation to environmental conditions. Nucleus size is positively correlated with genome size in vertebrates (Gregory 2001). Accordingly, the amount of DNA regulates the size of cells as well as the nucleus. Larger nuclei have more room for protein synthesis that are required in the metabolism of larger cells (Gregory 2001). Variations in RBC DNA content are also directly related to hematopoiesis, which in turn influence species adaptation. Genome

size seems also related to life-history traits. For example, genome size is positively related with the size and diameter of eggs, and negatively related with growth rate and standard size in fish (Hardie and Hebert, 2004; Smith and Gregory 2009).

The shape of RBC also changes according to cell maturation stage. While immature RBC (erythroblasts) are usually rounded, older cells are fusiform (Fijan 2002, Passantino et al. 2004). However, the degree of ellipticalness seems to vary among species (Dal'Bó et al., 2015). However, little is known about the physiological implications of the variation in the fusiform shape for species. Similarly, little is known about the factors involved in the variation of RBC volume and its implications (Lay and Bladwin 1999) but increasing temperature and body mass increase RBC volume in tetrapods (Gillooly and Zenil-Ferguson 2014). Also, RBC volume is related to polyploidy in fish (Gregory 2001). However, little is known about the relative role of phylogenetic relationships and abiotic factors in determining RBC shape.

No study has yet analysed how RBC shape have evolved in fish using modern phylogenetic comparative methods. As shape is multivariate, here we used a set of first- and second-order stereological variables to describe the shape of RBC. Also, we tested if the position in the water column, as a proxy for partial oxygen pressure, species are usually found affect RBC shape. Our hypothesis is that neustonic species (that live closer to the surface) would have smaller RBC due to higher surface area to volume ratio. We also built the phylomorphospace of RBC shape and tested for phylogenetic signal. We expect species with similar habitat use would be close together in the morphospace. This is the first study combining common stereological analysis and phylogenetic comparative method to understand how fish RBC evolved. Our results can help understand how fish species evolved to occupy habitats with different oxygen

concentration or toxicity, besides understanding how metabolic rate vary among species.

Methods

Specimen sampling

We analyzed five individuals of 15 species belonging to 15 genera and 2 superorders: *Pygocentrus nattereri*, *Gymnotus inaequilabiatus*, *Astyanax lineatus*, *Bujurquina vittata*, *Cichlasoma dimerus*, *Metynnis maculatus*, *Prochilodus lineatus*, *Piaractus mesopotamicus*, *Rhamdia quelen*, *Poecilia reticulata*, *Hypostomus boulengeri*, *Pseudoplatystoma corruscans*, *Synbranchus marmoratus*, *Brycon hilarii*, and *Hyphessobrycon anisitsi* (Figure 1). We obtained adult fish specimens from both sexes between 2017 and 2018 from a number of sources: *Pygocentrus nattereri* was fished in a river the Pantanal field station (Corumbá, Mato Grosso do Sul, central Brazil); *Gymnotus inaequilabiatus*, *Hyphessobrycon anisitsi*, and *Synbranchus marmoratus* were bought from a fish store; *Astyanax lineatus* and *Bujurquina vittata* were collected in an urban lake in Campo Grande; *Cichlasoma dimerus*, *Metynnis maculatus*, *Prochilodus lineatus*, *Piaractus mesopotamicus* were donated by the city aquarium; *Pseudoplatystoma corruscans*, Brycon hilarii, and *Hypostomus boulengeri* were obtained from the university Aquaculture Research ponds; *Poecilia reticulata* was collected in an urban stream in Campo Grande. These species were selected because they are common in our region, use distinct habitats, and belong to distant lineages.

Fish were anaesthetized with eugenol solution (50 mg L^{-1}) before blood sampling. Blood was collected by caudal vein or cardiac puncture with syringe with 3% EDTA or by decapitation in small species (Ranzani-Paiva et al., 2013). Blood smears were stained with May-Grunwald-Giemsa-Wright for erythrocyte morphometry

(Tavares-Dias and Moraes 2002). Detailed protocol is available at Rodrigues et al. (2020; see also Figure S1).

Red blood cell stereology

Design-based stereological methods have been used since the 1970s to quantify shape and size changes in cells and histological structures (West 2012). This approach uses linear (first-order) measurements to derive tridimensional (second-order) variables that describe the shape of cells in tissues. To take measurements, we used a digital camera (Nikon D3500) coupled in a light microscopy (Zeiss Primo Star®). Digital images in 1000x magnification were used to measure the following first-order variables: area (μm^2), perimeter, and largest and smallest diameter (µm) of cells and area, perimeter, and diameter of the nucleus in 50 randomly selected cells per animal (see Supporting material), i.e., 250 cells per species (50 cells * 5 animals). From these linear measurements, we calculated the following second-order stereological measurements: To calculate length, we took the mean of the largest and smallest diameters. Then, to calculate radius, we simply divided length by 2. Cell volume (μm^3) was calculated using the formula:

$$\frac{4}{3\pi} r^3$$

, where r is radius (see West 2012); nucleus volume (μm^3) was calculated by the formula:

$$\frac{CV * N{:}C}{100}$$

, where CV is cell volume and N:C is nucleus:cytoplasm ratio. Cell and nucleus circularity (or shape factor) were estimated by the formula:

$$\frac{4\pi A}{P^2}$$

, where *A* is cell area and *P* cell perimeter (Russ and Dehoff 2000). Circularity ranges from 0 (elliptical shape) to 1 (circular shape). All measurements were made in Motic Images Plus 2.0 in a double-blind fashion (see Fig. S2).

We calculated the mean of each variable for each species (Table S1), which were used as phenotypic traits in further analysis. To visualize the correlation pattern between variables, we built a correlogram considering the average of each variable (Fig. S3) using the *corrplot* package (Wei and Simko, 2017) of R software.

Phylogenetic comparative methods

To carry out the comparative analyzes, we first obtained a phylogeny with branch length in millions of years representing the relationship of the 15 species for which we have phenotypic data (Figure 1). This phylogeny was obtained from a fully-sampled topology for Actinopterygii recently published (Rabosky et al., 2018). Analysis was done in the fishtree package (Chang et al., 2019).

Then, we performed a phylogenetic Principal Components Analysis (pPCA) on the matrix of phenotypic data with the eight variables considering the phylogeny (Revell, 2009). The pPCA was performed using the correlation matrix of variables and assuming that traits have evolved according to a Brownian Motion (BM) model of evolution. The pPCA uses a **C** matrix that describes the variance-covariance structure between species given by the phylogeny and the evolutionary model (BM in this case) to obtain the Principal Components and species scores (see also Adams & Collyer 2019). Analysis was performed using the `phyl.pca` function of the phytools package (Revell, 2012).

From this exploratory analysis, we built a morphospace for all 15 species showing their similarity in relation to RBC shape. The analysis estimates the node

values using a Maximum Likelihood method. Finally, we built the phylomorphospace by projecting the phylogeny onto the morphospace built with the first two Principal Components, which allows us to explore how lineages occupied the morphospace as their traits evolved (Adams and Coller 2018, 2019). Analysis was performed using the `phylomorphospace` function of the phytools package.

Finally, we calculated a phylogenetic signal measure for multivariate data called K_{mult} (Adams, 2014) using all pPCs to avoid missing variation (Uyeda et al., 2015). This method allows calculating a statistic that measures how similar closely related species are in relation to their phenotypic measurements. Blomberg's K (Blomberg et al., 2003) is a measure widely used to measure phylogenetic signal for univariate data and ranges from 0 <K> 1. High phylogenetic signal (K>1) indicates that closely related species tend to be similar in relation to phenotypic attributes (Münkemüller et al., 2012). This method has been adapted for multivariate data recently (Adams, 2014), along with a Monte Carlo randomization procedure that allows testing the significance of the statistic. Analysis was performed with the `physignal` function of the geomorph package (Adams et al. 2020).

To test the effect of the position in the water column species usually occupy on RBC shape, we gathered data on depth range from FishBase (Froese and Pauly 2019) and treated it as a categorical variable, henceforth referred to as habitat. Thus, species were classified as demersal (n=4), pelagic (n=2), and benthopelagic (n=9). Afterwards, we compared the fit of evolutionary models to the eight pPCs. Specifically, we fit Pagel's lambda transformation, Brownian Motion, and Ornstein-Uhlenbeck models to data using the leave one out cross-validation of the penalized log-likelihood, as implemented in the `mvgls` function (Clavel and Morlon 2020) of the package mvMORPH (Clavel et al. 2015) including habitat as a predictor variable. Then, we

compared the model fit using the Extended Information Criterion (EIC), which showed that the best model was Brownian Motion (BM; Table S2). We built a phylogenetic Generalized Least Squares (Clavel and Morlon 2020) using BM to test the effect of habitat on RBC shape, with the Pillai's trace as test statistic and Type I Sum of Squares.

Finally, to test the hypothesis if a change in evolution rate is the mechanism allowing species to occupy different positions in the morphospace, we estimated tip-level evolution rate of RBC shape using phylogenetic ridge regression, as implemented in the RRphylo package (Castiglione et al. 2018). For this analysis we used all eight pPCs. This analysis also automatically finds nodes in which there was a rate shift. The R markdown dynamic document describing how analyses were conducted and associated data are available at FigShare (Martins et al. 2020).

Results

The shape of Red Blood Cells (RBC) of fish species studied varied from oval to ellipsoid and a rounded nucleus (Figure 2). Cell size varied by an order of magnitude, from the largest cell of *Synbranchus* to the smallest in *Poecilia*. The same phenomenon happened to cell volume (Fig. 3). Nucleus area varied from 7.45 μm^2 ($\pm$ 1.2 SD) in *Poecilia* to 27.30 μm^2 ($\pm$ 4.9 SD) in *Synbranchus*. Additionally, the range of intraspecific variation in some measurements varied among species. For example, cell volume had the highest standard deviation, while shape factor, nucleus area and cell perimeter seem to vary less within species (Table S1).

The pPC1 retained 66.1%, while pPC2 retained 21.4% of the variation in RBC shape. Cell and nucleus area, cell and nucleus perimeter, cell and nucleus volume were highly negatively correlated (> 0.84) with pPC1, whereas the nucleus:cytoplasm ratio was highly (-0.87) correlated with pPC2 (Table S2). Species positively correlated with

227 pPC1 had higher shape factor, whereas those negatively correlated had higher cell and
228 nucleus area, nuclear and cell perimeter, cell and nucleus volume, and
229 nucleus:cytoplasm ratio (Table S2). Species positively correlated with pPC2 had higher
230 cell perimeter, cell and nuclear area, whereas those negatively correlated had higher
231 nucleus:cytoplasm ratio, nucleus and cell volume, and nucleus area (Fig. S4).

232 The distribution of species in the phylomorphospace suggest that closely related
233 species do not have RBC with similar shape (Fig. 4). Accordingly, RBC shape does not
234 exhibit phylogenetic signal (K_{mult} = 0.6317; Effect size = 0.7863; P = 0.159). The low
235 effect size suggest phylogenetic signal is not concentrated in a few dimensions. To test
236 if only a subset of dimensions displays phylogenetic signal (see Adams & Collyer
237 2019), we re-run the analysis with only the first two pPCs. Results did not change (see
238 Martins et al. 2020). However, the morphospace suggest a non-stationary pattern in the
239 evolution of RBC shape, since most closely related species occupy distant positions, but
240 the position of siluriformes (*Pseudoplatistoma*, *Rhamdia*, and *Hypostomus*) mirror their
241 phylogenetic relationship in the upper part of the morphospace. Interestingly, the
242 Acanthopterygii included in our sampling: *Synbranchus*, *Poecilia*, *Bujurquina*, and
243 *Cichlosoma* had the most divergent pattern, occupying extreme positions in the
244 phylomorphospace, whereas species of Ostariophysi were more packed together. There
245 is a high divergence in RBC shape within Characiformes. Therefore, there seems to be a
246 variation in the pattern of RBC shape evolution at the level of higher order groups
247 (Superorders), instead of a homogeneous pattern throughout the whole phylogeny.

248 Habitat did not influence RBC shape (Pillai's trace=0.6936; P=0.461). The
249 results did not change if we use a multivariate PGLS (Table S4). We also found that
250 evolution rate of RBC shape was very heterogeneous at the tip level (Fig. 5). The
251 species with the highest rate was *Pygocentrus* (0.741) and the lowest was *Bujurquina*

(0.087). There was a tendency to increase the rate in the common ancestor of *Pygocentrus*, *Metynnis*, and *Piaractus* in relation to the background rate, but the rate shift was not significant (rate difference = 0.392; $P > 0.005$). Interestingly, the species occupying the most extreme positions in the phylomorphospace, such as *Synbranchus* (0.514), *Astyanax* (0.555), and *Gymnotus* (0.17) were not the ones with the highest rates of evolution. Therefore, our results suggest that an increase in the rate of evolution does not necessarily produces morphological specialization and rate disparity is not the main pattern involved in the formation of RBC morphospace.

Discussion

We found that the shape of Red Blood Cells (RBC) varies greatly among and within freshwater fish species. Contrarily to our initial hypothesis, we did not find a correlation between water column position (proxy for oxygen availability) and RBC shape. Accordingly, we did not find phylogenetic signal in RBC shape, suggesting closely related species do not have similar RBC shape. There does not seem to be a single mechanism driving the evolution of RBC shape, since the phylomorphospace shows a non-stationary pattern in the species similarity.

Small RBC allow species to occupy environments with low dissolved oxygen, since they usually have a higher number of cells, making them more efficient in oxygen uptake and transport (Silkin et al., 2019; Hawkey et al., 1991). Species with RBCs that have large surface area and volume have low metabolic rate, since the cell surface:volume ratio decreases the metabolic cost of gas exchange between membranes (Jones 1979, Lay and Baldwin, 1999). *Synbranchus* had higher perimeter (i.e., higher surface) and higher area. Thus, our results suggest that this species could have a lower metabolic rate than *Poecilia*, because the later has a smaller cell area and perimeter.

Most species occupied the center of the morphospace, independent of the phylogenetic relationship. This clustering of distantly related species suggests that convergence, apparently not caused by water column position, could be a mechanism influencing RBS shape evolution (Adams and Collyer 2019). Clustering in morphospace can also suggest a developmental constraint (Jablonski 2020) that impedes species to change their traits after speciation (Pie and Weitz 2005). Also, a few species were in extreme positions. Even though water column position did not explain RBC shape, the extreme position of *Synbranchus*, *Astyanax*, and *Poecilia* in the morphospace could be explained by differences in their life history strategies. For example, *Synbranchus* displays facultative pulmonary respiration, usually occurs in habitats with hypoxia, and burry itself during the dry season (Froese and Pauly, 2019). *Astyanax* also occurs in habitats with hypoxia (Froese and Pauly, 2019). The pattern we found points to clade disparity differences (Adams & Collyer 2019), with Acanthopterygii having higher dispersion in the morphospace than Ostariophysi (Fig. S6). These two orders have different ecological and biogeographic characteristics. Species from Ostariophysi are essentially from freshwater, while Acanthopterygii has marine origins, with secondary freshwater introgressions. One interesting pattern that emerges from the morphospace is that apparently there is no constrains in the morphospace, because almost all regions have one species. Siluriformes seem to have similar RBC shape, given their position in the morphospace, and similar evolution rate. This lineage occupies the upper position of the morphospace, along with *Piaractus* and *Hyphessobrycon*, and had high cell area and perimeter, and low nucleus:cytoplasm ratio, nucleus volume, and circularity. Exception for *Rhamdia* and *Hyphessobrycon*, all those species are demersal (benthic). Together these results suggest that the evolution of

RBC shape was driven by fluctuating selection, although this result should be taken with care, since our sample size is not large.

We found a high heterogeneity in evolution rate of RBC shape. This high rate heterogeneity helps explain why we did not detect a significant phylogenetic signal, i.e., the change in shape seems to vary strongly at the tip level, instead of large clades. This is consistent with the model selection procedure that pointed Brownian Motion (BM) as best fit model to the data. BM can be caused by genetic drift, when selection randomly varies in direction through time, or when selection is weak compared to the time scale analysed (Felsenstein 1988). The large intraspecific variation in most variables (Table S1) may suggest that variables describing RBC shape are under weak selection pressure (Nikinmaa 2019). Interestingly, the position extreme positions of *Synbranchus* (0.514), *Astyanax* (0.555), and *Pygocentrus* (0.741) could be explained at least partially by an increase in evolution rate, which allowed them to diverge from their sister species, remaining Acanthopterygii, *Hyphessobrycon*, and *Metynnis* respectively. However, given our sample size we cannot rule out that RBC shape of these species are evolving under directional selection. Conversely, if lineages followed a random walk (akin of BM) one would expect species to diverge and occupy positions in the morphospace irrespective of their habitat or phylogenetic position (Pie and Weitz 2005).

Water column position did not explain RBC shape in this freshwater fish species radiation. This result suggest that RBC shape may not be entirely determined by partial pressure of dissolved oxygen in water. It also suggests that water column position does not represent a main constraint in the evolution of these traits. A recent study (Minias 2020) also found that life history traits did not explain hemoglobin and hematocrit evolution in birds. Differently from mammals, fish RBC are nucleated cells and have many cytoplasmic organelles, such as mitochondria, Golgi complex, centrioles,

ribosomes, microtubules, rough and smooth endoplasmic reticulum (Sekhon and Beams 1969), as well as a range of cytoplasmatic enzymes involved in the anaerobic glycolysis (Sephton et al. 1991). These organelles and enzymes allow the functions of RBC to be finely regulated and somewhat independent from other components of the hematopoietic system, enabling fish to occupy a wide range of environments (Nikinmaa et al. 2019). Therefore, species may respond rapidly to changes in oxygen availability (Witeska, 2013), which indicates that it is not constrained by inheritance (Arnold 1992) or phylogenetic inertia, at least to a certain degree.

In conclusion, our study provides a novel macroevolutionary perspective on fish RBC shape by combining commonly used design-based stereological techniques with modern phylogenetic comparative methods. We found that the RBC of the two main orders of Neotropical freshwater fish vary greatly in shape, but that their water column alone does not explain it. Future studies should use quantitative genetic approaches to explore the underlying genetic basis for RBC morphology, possibly using geometric morphometrics and experimental approaches motivated by ecological data.

Acknowledgements

This study was supported by Universidade Federal de Mato Grosso do Sul – UFMS/MEC – Brasil. This study was funded in part by the Coordenação de Aperfeiçoamento de Pessoal de Nível Superior – Brasil (CAPES) – Finance Code 001. F. R. Carvalho and K. Tondato provided insightful comments as members of BOM bachelor's honors thesis examining committee.

Literature cited

Adams, D. C. 2014. A generalized K statistic for estimating phylogenetic signal from shape and other high-dimensional multivariate data. Syst Biol 63:685-697.

355 Adams, D. C., M. L. Collyer, and A. Kaliontzopoulou. 2020. Geomorph: Software for
356 geometric morphometric analyses. R package version 3.2.1. https://cran.r-
357 project.org/package=geomorph.
358 Adams, D. C. and M. L. Collyer. 2018. Multivariate Phylogenetic Comparative Methods:
359 Evaluations, Comparisons, and Recommendations. Syst Biol 67:14-31.
360 Adams, D. C. and M. L. Collyer. 2019. Phylogenetic Comparative Methods and the Evolution
361 of Multivariate Phenotypes. Annual Review of Ecology, Evolution, and Systematics 50:
362 405-425.
363 Anderson, H. L., I. E. Brodsky, N. S. Mangalmurti. 2018. The Evolving Erythrocyte: Red
364 Blood Cells as Modulators of Innate Immunity. *Journal of Immunology* 201: 1343-
365 1351.
366 Arnold, S. J. 1992. Constraints on phenotypic evolution. Am Nat 140 Suppl 1:S85-107.
367 Blomberg, S. P., T. Garland, Jr., and A. R. Ives. 2003. Testing for phylogenetic signal in
368 comparative data: behavioral traits are more labile. Evolution 57:717-745.
369 Castiglione, S., G. Tesone, M. Piccolo, M. Melchionna, A. Mondanaro, C. Serio, M. Di
370 Febbraro, P. Raia, and N. Cooper. 2018. A new method for testing evolutionary rate
371 variation and shifts in phenotypic evolution. Methods in Ecology and Evolution 9:974-
372 983.
373 Chang, J., D. L. Rabosky, S. A. Smith, M. E. Alfaro, and D. Silvestro. 2019. An R package and
374 online resource for macroevolutionary studies using the ray□finned fish tree of life.
375 Methods in Ecology and Evolution 10:1118-1124.
376 Clavel, J., G. Escarguel, G. Merceron, and T. Poisot. 2015. mvmorph: an R package for fitting
377 multivariate evolutionary models to morphometric data. Methods in Ecology and
378 Evolution 6:1311-1319.

379 Clavel, J. and H. Morlon. 2020. Reliable Phylogenetic Regressions for Multivariate
380 Comparative Data: Illustration with the MANOVA and Application to the Effect of Diet
381 on Mandible Morphology in Phyllostomid Bats. Syst Biol.
382 Dal'Bó, G.A., Sampaio, F.G., Losekann, M.E., Queiroz, J.F.D., Luiz, A.J. B., Wolf, V.H.G.,
383 Gonçalves, V.T. and Carra, M.L. 2015. Hematological and morphometric blood value
384 of four cultured species of economically important tropical foodfish. Neotropical
385 Ichthyology 13:439-446.
386 Felsenstein, J. 1988. Phylogenies and Quantitative Characters. Annual Review of Ecology and
387 Systematics 19:445-471.
388 Fijan, N. 2002. Morphogenesis of blood cell lineages in channel catfish. *Journal of fish biology*
389 60: 999-1014.
390 Froese, R. and D. Pauly. 2019. FishBase. World Wide Web electronic publication.
391 Gillooly, J. F. and R. Zenil-Ferguson. 2014. Vertebrate blood cell volume increases with
392 temperature: implications for aerobic activity. PeerJ 2:e346.
393 Glomski, C. A., Tamburlin, J., Chainani, M. 1992. The phylogenetic odyssey of the
394 erythrocyte. III. Fish, the lower vertebrate experience. *Histology and histopathology* 7:
395 501-28.
396 González-Morales, J. C., R. Beamonte-Barrientos, E. Bastiaans, P. Guevara-Fiore, E. Quintana,
397 and V. Fajardo. 2017. A Mountain or a Plateau? Hematological Traits Vary Nonlinearly
398 with Altitude in a Highland Lizard. *Physiological and Biochemical Zoology* 90: 638-
399 645.
400 Graham, M.S., Haedrich, R.L. and Fletcher, G.L. 1985. Hematology of three deep-sea fishes: A
401 reflection of low metabolic rates. Comparative biochemistry and physiology. A,
402 Comparative physiology 80:79-84.

403 Gregory, T. R. 2001. The bigger the C-value, the larger the cell: genome size and red blood cell
404 size in vertebrates. Blood Cells, Molecules, and Diseases 27:830-843.
405 Hawkey, C., P. Bennett, S. Gascoyne, M. Hart, and J. Kirkwood. 1991. Erythrocyte size,
406 number and haemoglobin content in vertebrates. British journal of haematology 77:392-
407 397.
408 Hardie, D.C. and Hebert, P.D. 2003. The nucleotypic effects of cellular DNA content in
409 cartilaginous and ray-finned fishes. Genome 46:683-706.
410 Jablonski, D. 2020. Developmental bias, macroevolution, and the fossil record. Evolution &
411 development 22:103-125.
412 Jones, D. 1979. The important of surface area/volume ratio to the rate of oxygen uptake by red
413 cells. The Journal of general physiology 74:643-646.
414 Lay, P. A. and J. Baldwin. 1999. What determines the size of teleost erythrocytes? Correlations
415 with oxygen transport and nuclear volume. Fish Physiology and Biochemistry 20:31-35.
416 Kumar, M. V. 2016. Morphometric studies of blood cells in *Cyprinus carpio*,
417 *Ctenopharyngodan idella* and *Hypophthalmichthys molitrix* cultured fish in west
418 Godavari region of Andhra Pradesh. International Journal of Fisheries and Aquatic
419 Studies 4: 489-493.
420 Maciak, S., Janko, K., Kotusz, J., Choleva, L., Boroń, A., Juchno, D., Kujawa, R.,
421 Kozłowski, J. and Konarzewski, M. 2011. Standard Metabolic Rate (SMR) is
422 inversely related to erythrocyte and genome size in allopolyploid fish of the
423 *Cobitis taenia* hybrid complex. *Functional Ecology* 25: 1072-1078.
424 Martins, B. O.; Franco-Belussi, L.; Siqueira, M. S.; Fernandes, C. E. S.; Provete, D.
425 (2020): The evolution of red blood cell shape in a continental radiation of
426 fishes. figshare. Dataset. https://doi.org/10.6084/m9.figshare.12044325.v1

427 Minias, P. 2020. Ecology and evolution of blood oxygen-carrying capacity in birds.
428 American Naturalist 195. DOI: https://doi.org/10.1086/707720.
429 Münkemüller, T., S. Lavergne, B. Bzeznik, S. Dray, T. Jombart, K. Schiffers, and W.
430 Thuiller. 2012. How to measure and test phylogenetic signal. Methods in
431 Ecology and Evolution 3:743-756.
432 Nikinmaa, M. 1990. Vertebrate Red Blood Cells. Springer-Verlag, Berlin.
433 Nikinmaa, M. 2019. Environmental regulation of the function of circulating erythrocytes via
434 changes in age distribution in teleost fish: Possible mechanisms and
435 significance. Marine genomics 49:100717.
436 Nikinmaa, M., Berenbrink, M., & Brauner, C. J. 2019. Regulation of erythrocyte function:
437 multiple evolutionary solutions for respiratory gas transport and its regulation in fish.
438 Acta Physiologica 227:e13299.
439 Passantino, L., Altamura, M., Cianciotta, A., Jirillo, F., Ribaud, M.R., Jirillo, E., and
440 Passantino, G.F. 2004. Maturation of Fish Erythrocytes Coincides with Changes in their
441 Morphology, Enhanced Ability to Interact with Candida albicans and Release of
442 Cytokine□Like Factors Active Upon Autologous Macrophages. Immunopharmacology
443 and immunotoxicology 26:573-585.
444 Pie, M. R. and J. S. Weitz. 2005. A Null Model of Morphospace Occupation. American
445 Naturalist 166: E1-13.
446 Rabosky, D. L., J. Chang, P. O. Title, P. F. Cowman, L. Sallan, M. Friedman, K. Kaschner, C.
447 Garilao, T. J. Near, M. Coll, and M. E. Alfaro. 2018. An inverse latitudinal gradient in
448 speciation rate for marine fishes. Nature 559:392-395.
449 Ranzani-de-Paiva, M. J. T., de Pádua, S. B., Tavares-Dias, M., & Egami, M. I. 2013. Métodos
450 para análise hematológica em peixes. Editora da Universidade Estadual de Maringá-
451 EDUEM.

452 Revell, L. J. 2009. Size-correction and principal components for interspecific comparative
453 studies. Evolution 63:3258-3268.
454 Revell, L. J. 2012. phytools: an R package for phylogenetic comparative biology (and other
455 things). Methods in Ecology and Evolution 3:217-223.
456 Rodrigues, R. A., Siqueira, M. S., Martins, B. O., Fernandes, C. E., Franco-Belussi, L., Provete,
457 D.B. (2020). Staining of fish Red Blood Cells. **protocols.io**
458 dx.doi.org/10.17504/protocols.io.bd9yi97w
459 Russ, J.C., Dehoff, R.T. 2000. Practical stereology. 2nd ed. Springer science.
460 Szarski, H. 1970. Changes in the amount of DNA in cell nuclei during vertebrate evolution.
461 Nature 226:651-652.
462 Sekhon, S. S., Beams, H.W. 1969. Fine structure of the developing trout erythrocytes and
463 thrombocytes with special reference to the marginal band and the cytoplasmic
464 organelles. American Journal of Anatomy, 125:353-373.
465 Sephton, D. H., MacPhee, W. L., Driedzic, W. R. (1991). Metabolic enzyme activities, oxygen
466 consumption and glucose utilization in sea raven (Hemitripterus americanus)
467 erythrocytes. *Journal of experimental biology 159*: 407-418.
468 Silkin, Y. A., E. Silkina, V. Chernyaeva, and V. Vasilets. 2019. Study of Dimensional and
469 Morphological Characteristics of Erythrocytes in Some Black Sea Fish of Different
470 Evolution Position and Ecological Specialization. Journal of Ichthyology 59:97-103.
471 Smith, E. M. and T. R. Gregory. 2009. Patterns of genome size diversity in the ray-finned
472 fishes. Hydrobiologia 625:1-25.
473 Tavares-Dias, M., and de Moraes, F. R. 2006. Características hematológicas da *Tilapia rendalli*
474 Boulenger, 1896 (Osteichthyes: Cichlidae) capturada em "pesque-pague" de Franca,
475 São Paulo, Brasil. Bioscience Journal, 19: 107-114.

476 Uyeda, J. C., D. S. Caetano, and M. W. Pennell. 2015. Comparative Analysis of Principal
477 Components Can be Misleading. Syst Biol 64:677-689.
478 Wei, T., and Simko, V. “R package "corrplot": Visualization of a Correlation Matrix (Version
479 0.84)”. Available from https://github.com/taiyun/corrplot (2017).
480 West, M.J. 2012. Basic stereology for biologists and neuroscientists. Cold Spring harbor
481 laboratory press. New York.
482 Wintrobe, M.M. 1934. Variations in the size and hemoglobin content of erythrocytes in the
483 blood of various vertebrates. Folia haematologica 51:32-49.
484 Witeska, M. 2013. Erythrocytes in teleost fishes: a review. Zoology and Ecology 23:275-281.
485 Yakhnenko, V.M., Klimenkov, I.V., Sudakov, N.P. Belyshenko, A. Y., Glyzina, O. Y.,
486 Mamontov, A. M., Sapozhnikova, Y P. and Sukhanova, L. V. 2016. Morphofunctional
487 peculiarities of erythrocytes in wild and farmed Coregonid fishes from Lake Baikal.
488 *Contemporary Problems in Ecology* 9**:** 219–228

489
490 Figure Legends
491
492 Figure 1. Dated phylogenetic tree with species to which we have phenotypic data used
493 in the analysis, pruned from Rabosky et al. (2018).
494
495 Figure 2. Shape and size of Red Blood Cells of the 15 fish species analysed. Staining:
496 MMGW. Scale bars = 10 µm.
497
498 Figure 3. Diagram showing the mean of each stereological variable with the
499 phylogenetic tree of the species sampled. Data on standard deviation for each variable is
500 available at Table S1.
501
502 Figure 4. Phylomorphospace constructed with phylogenetic Principal Components 1
503 and 2 showing species distribution in the reduced space. Red Blood Cell (RBC) images
504 are all in the same magnification and belong to species occupying the extreme positions
505 along each pPC. The RBC associated positively with pPC1 is from *Poecilia*, which has
506 a high shape factor, while the RBC associated negatively with pPC1 is from
507 *Synbranchus* that has high cell area and perimeter, and high nucleus area and perimeter.
508 The RBC associated positively with pPC2 belongs to *Pseudoplatystoma*, which has high
509 cell perimeter. The RBC image associated negatively with pPC2 is from *Astyanax* and
510 has a high shape factor, high nucleus:cytoplasm ratio, and high nucleus volume. Colours
511 represent depth in the water column species are usually found, green = Pelagic; black =
512 Benthopelagic; red = Demersal.

Figure 5. Phylogenetic tree showing the results of the tip-level evolution rate estimated using ridge regression for the stereological variables describing the Red Blood Cell shape. Analysis was conducted in RRphylo.

Data accessibility statement

All the data and R code used to run the analysis will be deposited in FigShare upon acceptance.

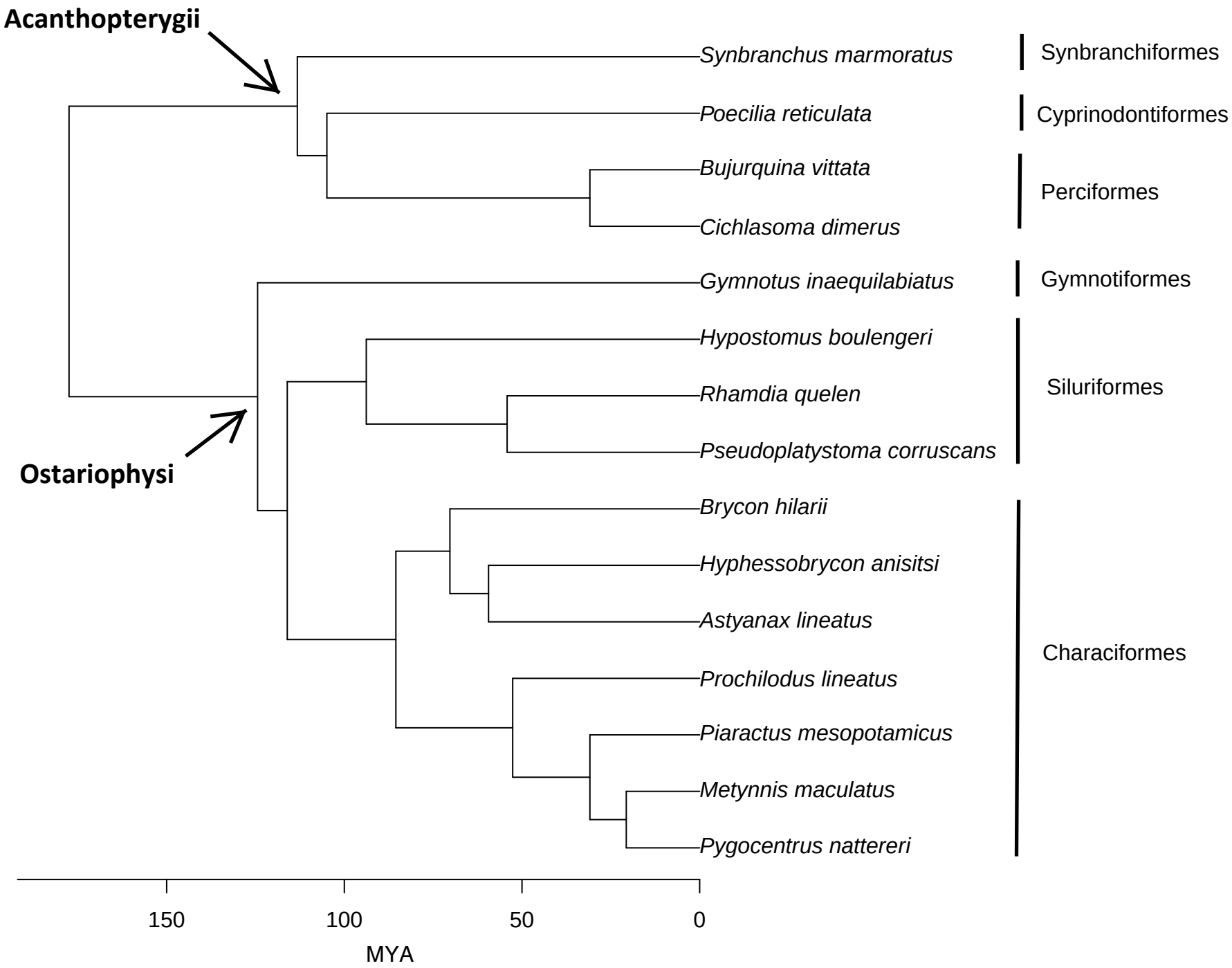
Acanthopterygii
Ostariophysi
Synbranchus marmoratus
Poecilia reticulata
Bujurquina vittata
Cichlasoma dimerus
Gymnotus inaequilabiatus
Hypostomus boulengeri
Rhamdia quelen
Pseudoplatystoma corruscans
Brycon hilarii
Hyphessobrycon anisitsi
Astyanax lineatus
Prochilodus lineatus
Piaractus mesopotamicus
Metynnis maculatus
Pygocentrus nattereri
Synbranchiformes
Cyprinodontiformes
Perciformes
Gymnotiformes
Siluriformes
Characiformes
150
100
50
0
MYA

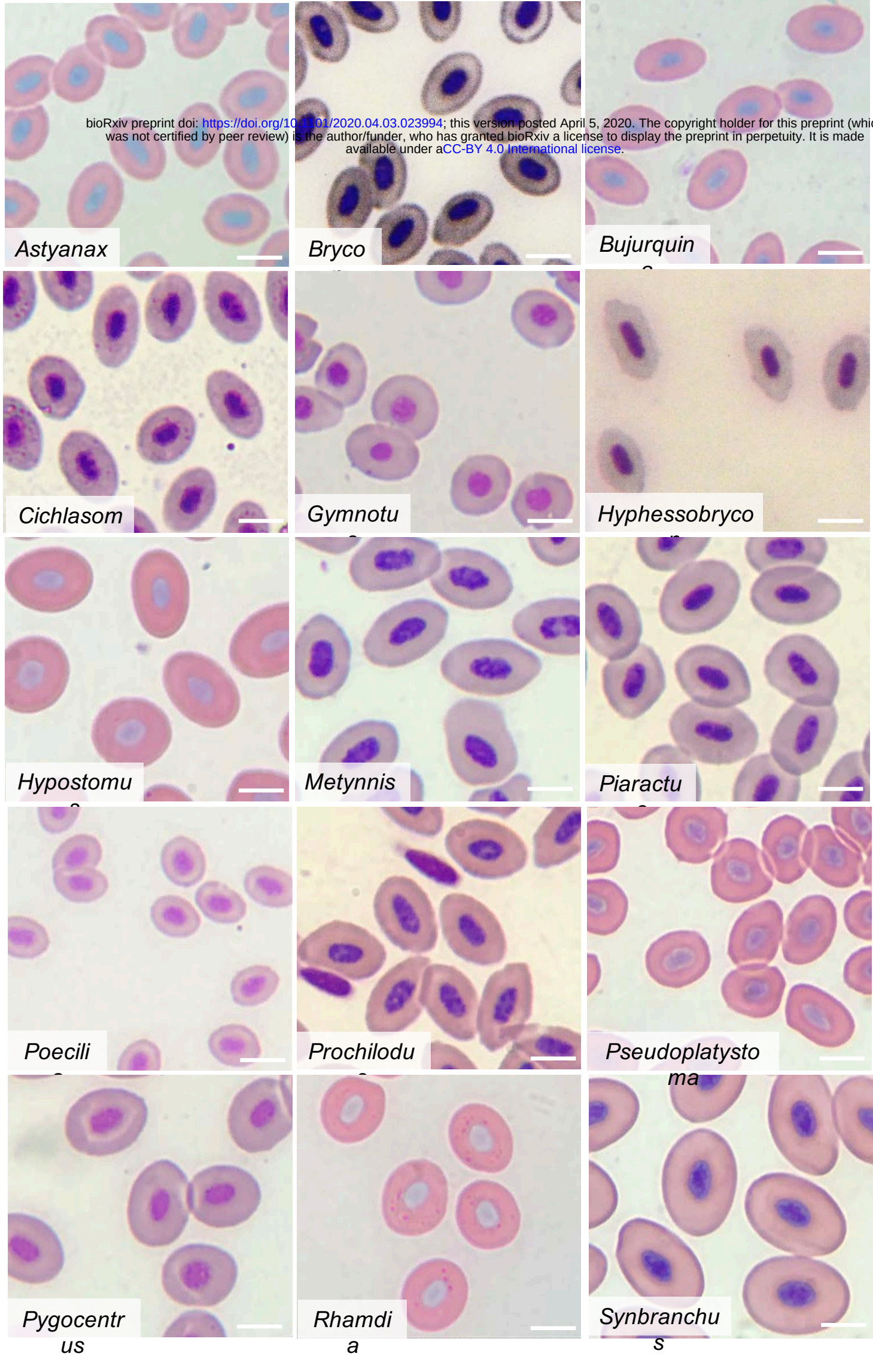

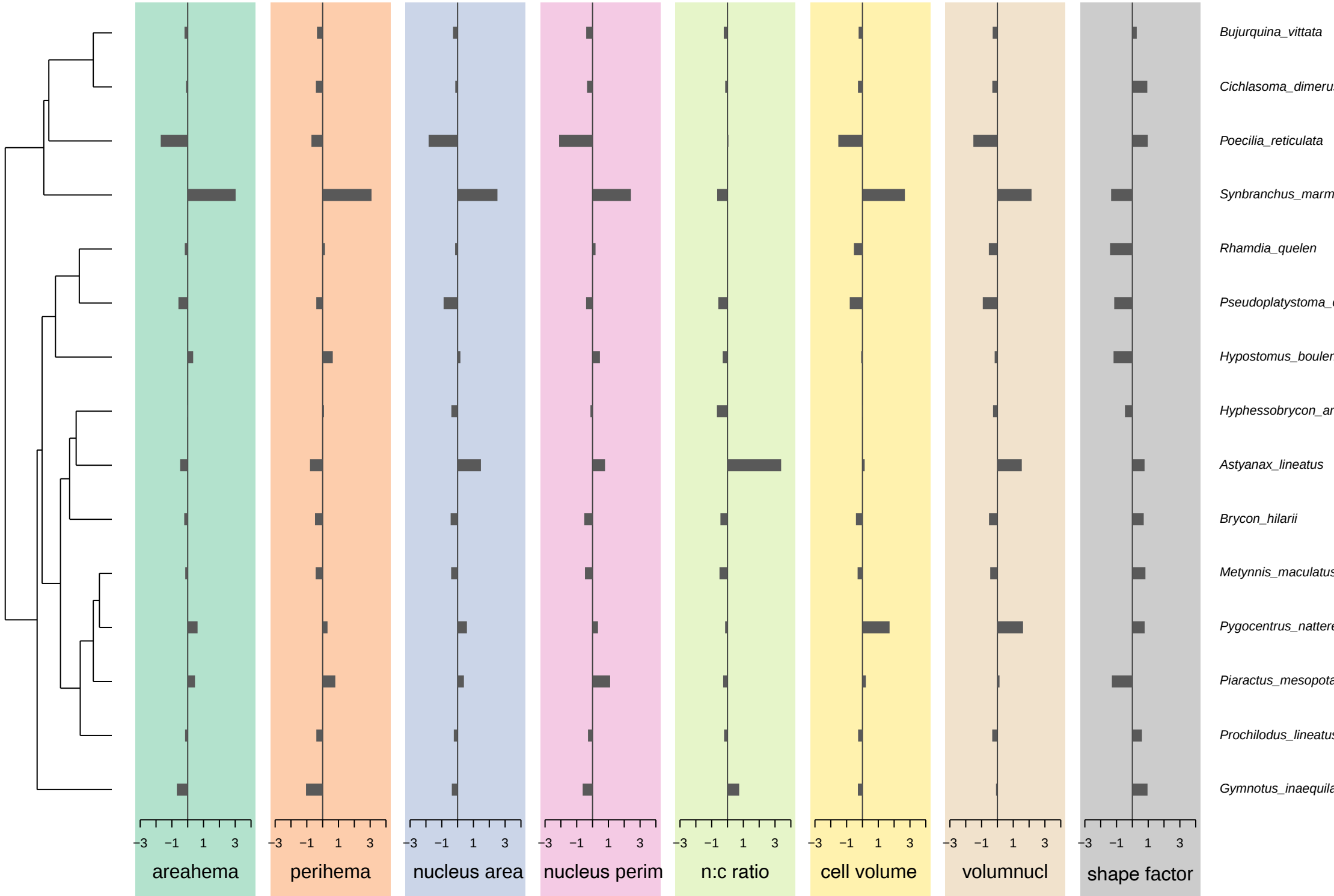
Bujurquina_vittata
Cichlasoma_dimeru
Poecilia_reticulata
Synbranchus_marm
Rhamdia_quelen
Pseudoplatystoma_
Hypostomus_boulen
Hyphessobrycon_ar
Astyanax_lineatus
Brycon_hilarii
Metynnis_maculatus
Pygocentrus_nattere
Piaractus_mesopota
Prochilodus_lineatus
Gymnotus_inaequila
−3 −1 1 3
areahema
perihema
nucleus area
nucleus perim
n:c ratio
cell volume
volumnucl
shape factor

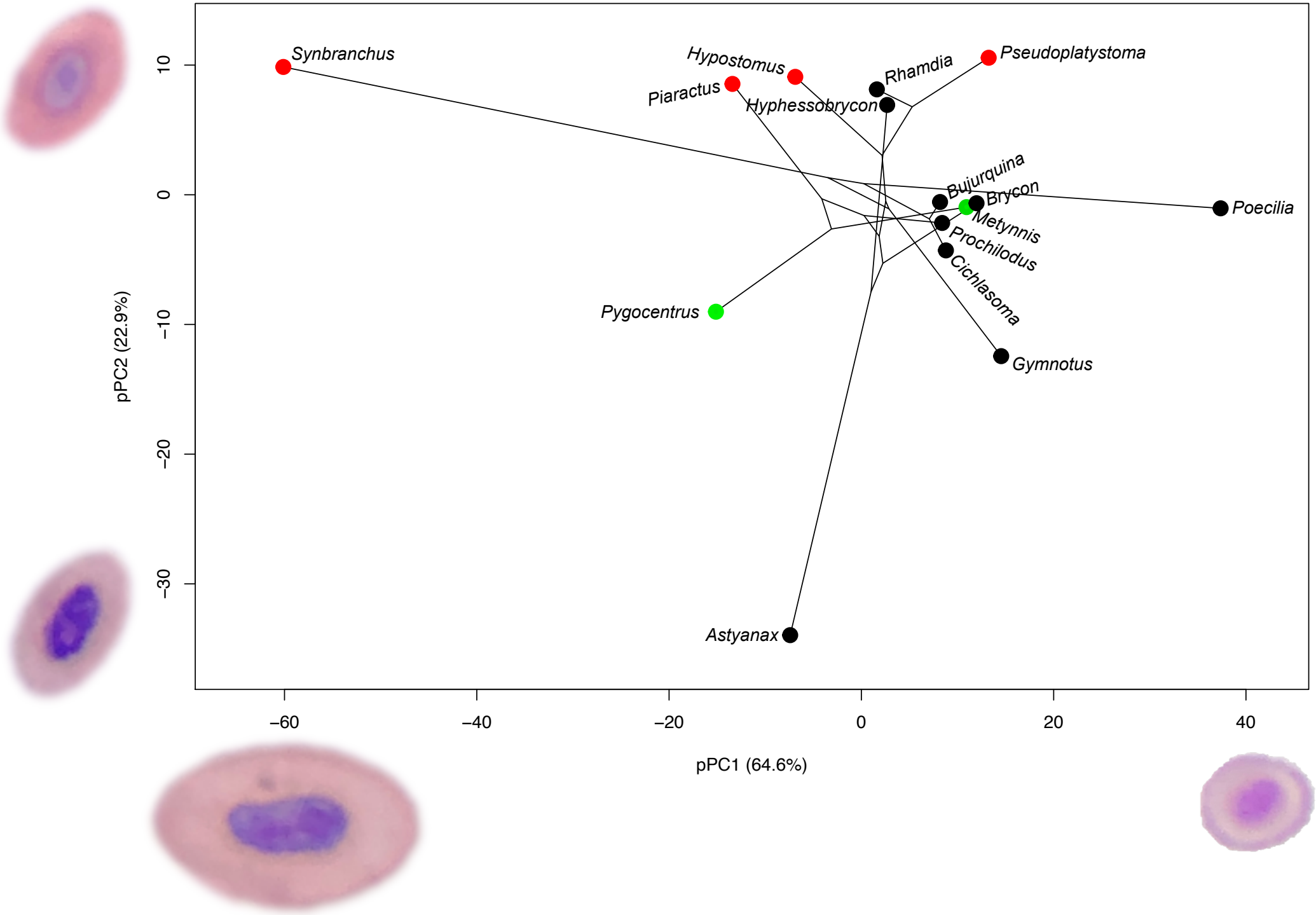
Synbranchus
Hypostomus
Piaractus
Hyphessobrycon
Rhamdia
Pseudoplatystoma
Bujurquina
Brycon
Metynnis
Prochilodus
Cichlasoma
Poecilia
Pygocentrus
Gymnotus
Astyanax
10
0
−10
−20
−30
pPC2 (22.9%)
−60
−40
−20
0
20
40
pPC1 (64.6%)

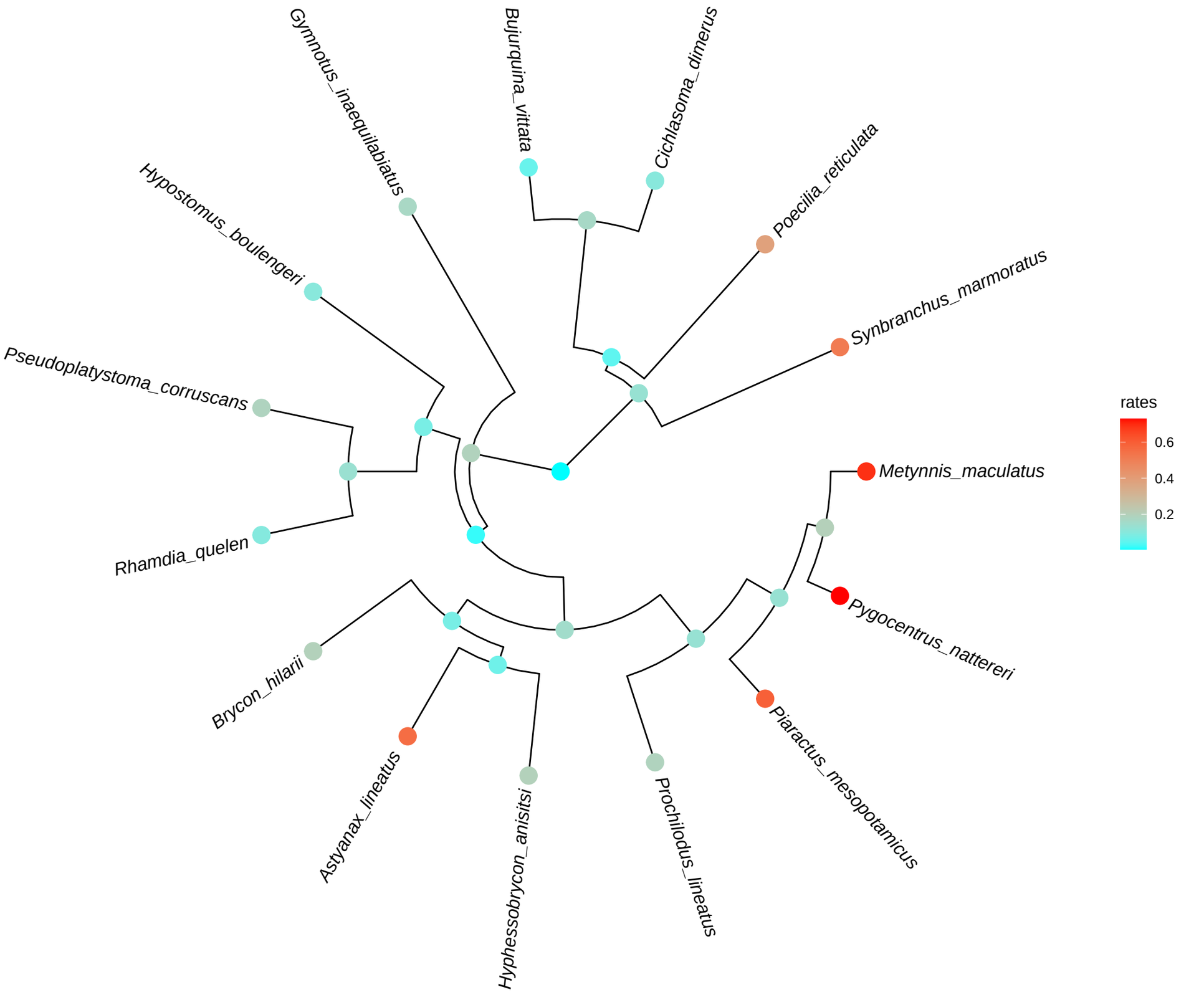
Gymnotus_inaequilabiatus
Bujurquina_vittata
Cichlasoma_dimerus
Poecilia_reticulata
Synbranchus_marmoratus
Hypostomus_boulengeri
Pseudoplatystoma_corruscans
Rhamdia_quelen
Metynnis_maculatus
Pygocentrus_nattereri
Piaractus_mesopotamicus
Brycon_hilarii
Astyanax_lineatus
Hyphessobrycon_anisitsi
Prochilodus_lineatus
rates
0.6
0.4
0.2